

Quantitative MR System Evaluation Using the KMRP-4 Phantom - Comparison with the ACR Phantom

Jong-Min Kim¹, Jang-Gyu Cha², Ji-Young Hwang³, Seung-Eun Jung⁴, Hyunn-Kyoon Lim⁵, Do-wan Kim⁶, Kwang-Su Kim⁶, Sung-Jin Kang², Han-Joong Kim¹, Suchit Kumar¹, Junyong Park⁷, Chulhyun Lee⁷, and Chang-Hyun Oh¹

¹Electronic and information engineering, Korea University, Seongbuk-Gu, Seoul, Korea, ²Department of Radiology, Soonchunhyang University Bucheon Hospital, Seoul, Korea, ³Department of Radiology, Ewha Women's University Mokdong Hospital, Seoul, Korea, ⁴Department of Radiology, The Catholic University of Korea St. Mary's Hospital, Seoul, Korea, ⁵Korea Research Institute of Standards and Science, Daejeon, Korea, ⁶Korean Institute of Accreditation of Medical Imaging, Seoul, Korea, ⁷The MRI Team, Korea Basic Science Institute, Chungcheongbuk-do, Korea

TARGET AUDIENCE: MR physicists, clinicians, radiologists interested in MRI quality evaluation using phantoms

PURPOSE: The quality evaluation scheme using the ACR phantom¹ is good enough to decide whether the MRI system is useful for clinical application based on certain measurement parameters showing the image quality. Using the ACR phantom, a total of 11 planes of MR images are usually acquired and are used to evaluate the 7 features, namely, the geometric accuracy, high-contrast spatial resolution, slice thickness accuracy, slice position accuracy, image intensity uniformity, percent-signal ghosting, and low-contrast object detectability. There are, however, several limitations of ACR method such as observer-dependent and time consuming evaluation process which leads to an inaccurate numerical ratings on the system performance. In this study, we have designed, constructed, and tested a new phantom called KMRP-4 with some easier evaluation capabilities including the three items (vessel conspicuity, brain tissue contrast, SNR). More than 30 MR systems from 0.3 to 3.0 T from 5 vendors have been tested. For semi-automatic and quantitative MR system classification, all the above-mentioned items are evaluated numerically by using MATLAB (Mathwork, Inc., MA).

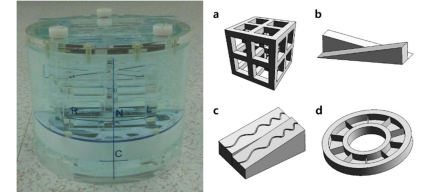


Figure 1 A photograph (left) and its inserts (right) of the KMRP-4 phantom (including the cubic (a), triangle (b), vessel (c), and low-contrast tissue (d) structure)

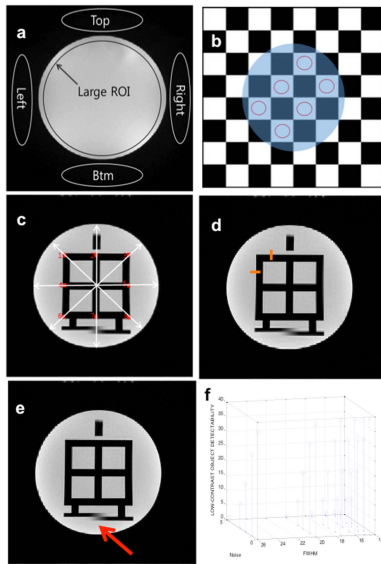


Figure 3 Typical reference MR images for the MRI system evaluation using the KMRP-4 phantom

METHODS: The KMRP-4 phantom has a cylindrical shape (diameter: 170 mm, length: 148 mm) with the inserts of cubic, triangular, vessel, and low-contrast tissue structures (Fig. 1). Slice position accuracy and percent-signal ghosting (Fig. 3a) are evaluated by using ACR method. Image intensity uniformity and SNR are estimated from Percent Intensity Uniformity and SNR, respectively, measured in the squares where all the elements are nonzero among the white 10-by-10 squares in the chessboard pattern (Fig. 3b). Geometry accuracy is evaluated by measuring the distance between the edges of cubic structure (Fig. 3c). The ratings on the high-contrast spatial resolution are estimated by analyzing the image of a phantom containing a cubic structure. The edges of the structure are used to calculate the resolution by differentiation and calculating the Full Width at Half Maximum (FWHM) along the vertical and horizontal directions. Slice thickness accuracy is measured by differentiating the slice profile along the horizontal line in the triangular structure and measuring FWHM divided by tangent of triangular structure (Fig. 3e). Low-contrast object detectability is strongly dependent on high-contrast spatial resolution and SNR. This item is computed by using model formula calculated by numerical simulation (Fig. 3f). Vessel conspicuity is evaluated by integrating the pixel value vertically for each column and by taking the 2nd order derivative horizontally, and then counting the number of peaks for the vessel areas. Brain tissue contrast is estimated by calculating the T₂ map and measuring the mean pixel value for each ROI having different agarose density placed along low-contrast tissue structure. For image acquisition, multi-echo sequence were used (an Achieva 3.0 T system from Philips and a 1.5 T Signa HDxt from GE Healthcare) with TEs of 20 & 80 msec, TR = 2 sec, Field Of View (FOV) = 250x250 mm², matrix size = 256x256, NEX = 1, slice thickness = 5 mm, gap = 5 mm, and number of slices = 11.

RESULTS: Figure 4a shows the comparison between ACR and KMRP-4 method for the geometric accuracy test, where the diameter of the circular uniform regions are 190 mm and 170 mm, for the ACR and KMRP-4 phantoms, respectively. The comparison results in Fig. 4b for the other six items show that more accurate quantitative evaluation is possible using KMRP-4 methods. Figures 5a and 5b show the good and bad image quality for the vessel conspicuity, where less number of peaks means better accuracy. Figure 6 shows that the mean pixel value decreases in the given ROI as the agarose concentration increases.

DISCUSSIONS AND CONCLUSIONS: Using the KMRP-4 method, in addition to the more stable evaluation of 7 items for the ACR phantom, evaluation of vessel detectability, brain tissue contrast detectability, SNR became possible. Quantitative semi-automatic evaluation became possible as well. Several limitations of ACR method were overcome. While the conventional MR evaluation using the ACR phantom gives only pass/fail decisions, the evaluation method using the KMRP-4 method made it possible to evaluate the performance of MR system quantitatively without observer dependency enabling a solid and stable quality assurance.

REFERENCES

1. Phantom Test Guidance for the ACR MRI Accreditation Program, The American College of Radiology, 1891 Preston White Dr. Reston, VA 20191-4397. 2005.

Acknowledgements: This research was supported by the MEST-BMBF University Cooperation Programme (NRF-2006-2005137) and Brain Korea Plus Program through the National Research Foundation of Korea (NRF) funded by the Ministry of Science, ICT and Future Planning and the Brain Korea 21 Plus Program (2014) of the National Research Foundation of Korea (NRF).

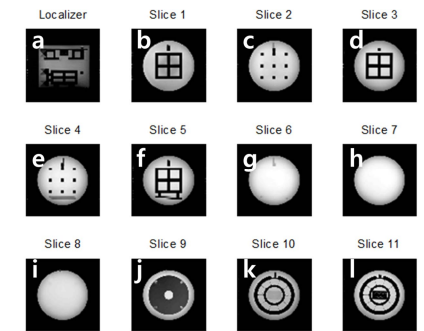


Figure 2 Multislice image of KMRP-4 phantom (cubic (a-f), uniform (h), vessel (i), and low-contrast tissue (i) structures)

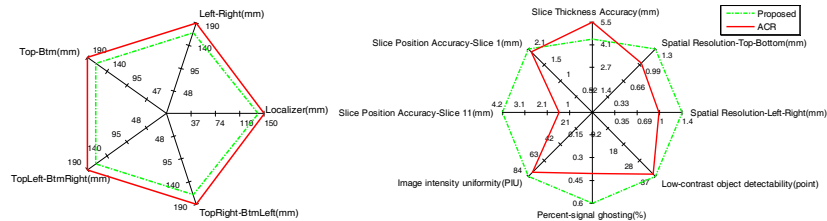


Figure 4a Comparison of geometric accuracy test of ACR and KMRP-4 method

Figure 4b Comparisons of other six items of ACR and KMRP-4 method.

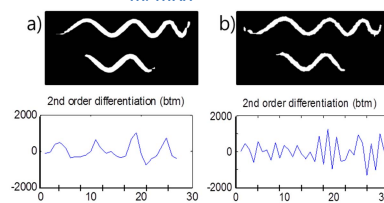


Figure 5 Comparison between good and bad imaging results for vessel conspicuity

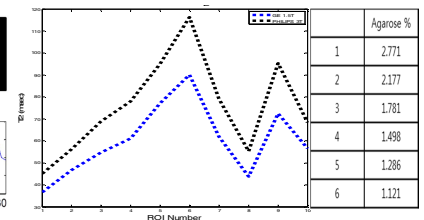


Figure 6 Calculated T₂ map and the corresponding agarose density.